Biochemical and Biophysical Research Communications 497 (2018) 869–875

Contents lists available at ScienceDirect

Biochemical and Biophysical Research Communications

journal homepage: www.elsevier.com/locate/ybbrc

Lis1 dysfunction leads to traction force reduction and cytoskeletal disorganization during cell migration

Guo-Wei Jheng [a], Sung Sik Hur [b], Chia-Ming Chang [a], Chun-Chieh Wu [a], Jia-Shing Cheng [a], Hsiao-Hui Lee [c], Bon-Chu Chung [d], Yang-Kao Wang [e], Keng-Hui Lin [f], Juan C. del Álamo [g], Shu Chien [b], Jin-Wu Tsai [a, h, *]

[a] Institute of Brain Science, School of Medicine, National Yang-Ming University, Taipei 112, Taiwan, ROC
[b] Department of Bioengineering and Institute of Engineering in Medicine, University of California at San Diego, La Jolla, CA 92093, USA
[c] Department of Life Sciences and Institute of Genome Sciences, School of Life Sciences, National Yang-Ming University, Taipei 112, Taiwan, ROC
[d] Institute of Molecular Biology, Academia Sinica, Taipei 11529, Taiwan, ROC
[e] Department of Cell Biology and Anatomy, College of Medicine, National Cheng Kung University, Tainan 70101, Taiwan, ROC
[f] Institute of Physics, Academia Sinica, Taipei 11529, Taiwan, ROC
[g] Department of Mechanical and Aerospace Engineering, University of California, La Jolla, San Diego, CA 92093, USA
[h] Brain Research Center (BRC) and Biophotonics and Molecular Imaging Research Center (BMIRC), National Yang-Ming University, Taipei 112, Taiwan, ROC

ARTICLE INFO

Article history:
Received 5 February 2018
Accepted 17 February 2018
Available online 20 February 2018

Keywords:
Traction force
Lis1
Migration
Microtubule
Actin
Focal adhesion

ABSTRACT

Cell migration is a critical process during development, tissue repair, and cancer metastasis. It requires complex processes of cell adhesion, cytoskeletal dynamics, and force generation. Lis1 plays an important role in the migration of neurons, fibroblasts and other cell types, and is essential for normal development of the cerebral cortex. Mutations in human *LIS1* gene cause classical lissencephaly (smooth brain), resulting from defects in neuronal migration. However, how Lis1 may affect force generation in migrating cells is still not fully understood. Using traction force microscopy (TFM) with live cell imaging to measure cellular traction force in migrating NIH3T3 cells, we showed that Lis1 knockdown (KD) by RNA interference (RNAi) caused reductions in cell migration and traction force against the extracellular matrix (ECM). Immunostaining of cytoskeletal components in Lis1 KD cells showed disorganization of microtubules and actin filaments. Interestingly, focal adhesions at the cell periphery were significantly reduced. These results suggest that Lis1 is important for cellular traction force generation through the regulation of cytoskeleton organization and focal adhesion formation in migrating cells.

1. Introduction

Cell migration is essential for many biological processes, such as embryonic development, tissue renewal, immunological responses, cancer metastasis, and wound healing [1–4]. Cell migration involves a series of dynamic processes, including polarization of the cell, formation of cell-matrix adhesions, protrusion of the cell front, translocation of the cell body, and retraction of the cell rear [5,6]. During this process, the traction force against extracellular matrix (ECM) is generated to modify the cell shape and to propel the cell forward. In eukaryotic cells, the contraction is generally produced by stress fibers, networks of actin filaments, and myosin II [7–9]. Typically, the traction forces are polarized according to the direction of motion of migrating cells.

LIS1, which consists of a WD40-repeat domain, a tryptophan-aspartic acid repeats, and an N-terminal LisH (Lissencephaly type-1-like homology) domain, interacts with the cytoplasmic dynein and its regulatory complex dynactin [10–12]. Mutations in *LIS1* gene were identified to cause classical (type I) lissencephaly [13], which is characterized by smooth or nearly smooth cerebral surface. We and others have demonstrated that Lis1 dysfunction induced by gene knockout or RNAi knockdown (KD) causes migration defects in cortical neurons, cerebellar granule cells, and fibroblasts [14–16]. In *Aspergillus*, mutations in homologues of LIS1, as well as cytoplasmic dynein and dynactin, inhibit nuclear migration within hyphal processes [17]; similarly, mutations in *Drosophila* Lis-1 cause defects in nuclear migration during

* Corresponding author. Institute of Brain Science, School of Medicine, National Yang-Ming University, No.155, Sec.2, Linong Street, Taipei 112, Taiwan, ROC.
E-mail address: tsaijw@ym.edu.tw (J.-W. Tsai).

https://doi.org/10.1016/j.bbrc.2018.02.151
0006-291X/

oogenesis [18]. Mutations in the yeast LIS1 homologue PAC1 lead to defects in nuclear orientation [19].

Although the role of Lis1 in cell migration was well established, its potential function in traction force generation has not been explored. The development of traction force microscopy (TFM) has allowed researchers to measure the forces that cells exert on the ECM [20–22]. In this study, we used RNAi to knock down Lis1 expression in NIH3T3 cells and showed that migration was markedly inhibited. We further measured the effect of Lis1 on cellular traction force and found that its KD dramatically reduced the traction force required for cell migration. To understand the underlying molecular mechanism, we investigated the change in the organization of microtubules, actin filaments and focal adhesion, and found that Lis1 KD affected the organization of each of these structures. These results suggest that Lis1 plays an important role in the generation of traction force, through regulating the organization of cytoskeleton and focal adhesion during cell migration.

2. Materials and methods

2.1. Constructs, cell culture and transfection

For RNAi, shRNA constructs based on the pRNAT-U6.1/Neo vector (GenScript), which expresses a GFP marker along with a shRNA, were used. Targeting sequences are shLIS1: GAGATGAACTAAATCGAGCTA and shCtrl: ATTGTATGCGATCGCAGACTT. The knockdown efficiency has been validated previously [14]. NIH3T3 cells (ATCC) derived from mouse embryo fibroblasts were maintained in Dulbecco's Modified Eagle's Medium (DMEM, pH = 7.3), supplemented with 10% (vol/vol) calf serum, 1% L-Glutamine, 100 U/ml penicillin and 100 μg/ml streptomycin, at 37 °C in humidified atmosphere with 5% CO_2. Plasmids were transfected into NIH3T3 cell by Lipofectamine 3000 reagent (L3000075, Invitrogen) according to the manufacturer's instructions. Briefly, 1 μg of plasmid was mixed with P3000 and Lipofetamine 3000 in Opti-MEM medium (31985070, Invitrogen) at room temperature for 10 min. Cells in serum-free medium were then incubated with the DNA-liposome complexes for 8 h. The serum-free medium was replaced by complete DMEM afterwards.

2.2. Cell motility assay

Cells were cultured on coverglass-bottom dishes coated with 100 μg/ml collagen and monitored on an inverted microscope (Axio Observer Z1, Zeiss) equipped with an on-stage incubator to maintain the samples at 5% CO_2 and 37 °C. Images were taken through a 10x objective lens (N.A. = 0.25) with AxioCam MRm CCD (Zeiss). Cell motility was analyzed by MTrackJ plugin [23] of ImageJ (NIH).

2.3. Polyacrylamide (PAA) gel fabrication

PAA gel fabrication was performed according to previous studies [21,24] with some modifications. Briefly, 5%/0.2% (vol/vol) acrylamide/bis-acrylamide solution was mixed with 0.1% ammonium persulfate (APS), 0.4% N,N,N′,N′-Tetramethylethylenediamine (TEMED) and 0.04% (vol/vol) 200 nm diameter fluorescent (580/605) polystyrene beads (F8810, Invitrogen) after degassing for 30 min at room temperature. 3 μl of the mixed solution was added onto the coverglass-bottom dish and sandwiched with a collagen-coated coverslip. The gel was allowed to polymerize for 1 h at 4 °C. The collagen was cross-linked with PAA gels surface by activated 1 mM sulfo-SANPAH (22589, Thermo Fisher Scientific) with UVB wavelength for 4 min twice. The gel was washed with 50 mM 4-(2-hydroxyethyl)-1-piperazineethanesulfonic acid (HEPES) on a shaker for 10 min three times. Collagen (20 μg/ml) was conjugated on PAA gels and incubated overnight at 4 °C. Cells were then cultured on the gel for 18 h and placed on a microscope for live cell imaging. The Young's modulus of the PAA gels was measured with rheometer (MCR 302, Anton Paar GmbH).

2.4. Live cell imaging

Fluorescence images of cells and beads were taken with an inverted epi-fluorescent microscope (Axio Observer Z1, Zeiss) equipped with an incubator to maintain the samples at 5% CO_2 and 37 °C. The images were taken through a 100× oil immersion objective lens (N.A. = 1.4) with AxioCam MRm CCD (Zeiss). Z-stack sections at 0.25-μm intervals for 51 slices were recorded every 10 min for 120 min. The reference bead images were obtained after the cells had been removed by treating with 0.1 M NaOH.

2.5. Traction force analysis

The traction force was analyzed based on particle image velocimetry (PIV) as described in a previous report [24] using programs written in Matlab (MathWorks). The window size was 32 × 32 pixels and the spatial resolution in x and y directions was 0.102 μm/px. Traction stress was solved with the finite element method using Abaqus software (Dassault Systèmes).

2.6. Immunocytochemistry

Cells were fixed for 15 min in 3% paraformaldehyde (PFA) and 1% glutaraldehyde. The cells were permeabilized in PBST solution (0.3% Triton X-100 in PBS, phosphate buffered saline) for 30 min and then blocked with 10% fetal bovine serum (FBS) in PBST solution (0.1% Triton X-100 in PBS) for 1 h at room temperature. Primary antibodies were used at following concentrations: mouse anti-alpha tubulin 1:500 (66031-1-Ig, Proteintech); rabbit *anti*-Lis1 1:100 (ab2607, Abcam). After incubation in primary antibody overnight at 4 °C, the cells were washed in PBS three times for 10 min. Alexa Fluor 488, 546, 647 (1:500) and Alexa Fluor 555 phalloidin (A34055, Invitrogen) were then applied for 2 h at room temperature. Finally, the coverslips were counterstained with 0.5 μg/ml DPAI (D1306, Invitrogen) for 30 min. VECTASHIELD® Mounting Medium Media was added before sealing the slides.

2.7. Confocal microscopy

Cellular structures were imaged under a laser scanning confocal microscope (LSM-700, Zeiss) with the 100× oil immersion objective lens (NA = 1.4). The excitation wavelengths were 405 nm for DAPI, 488 nm for GFP, 555 nm for Alexa Fluor 555/546, and 639 nm for Alexa Fluor 647. The Z-stack section was set at 0.25–1 μm.

2.8. Total internal reflection fluorescence (TIRF) microscopy

Focal adhesion was imaged under a TIRF microscope (Nikon) with a 60× oil immersion objective lens (NA = 1.4). The excitation wavelengths were 405 nm for DAPI, 488 nm for GFP, 550 nm for Cy3, and 649 nm for Cy5.

2.9. Statistical analysis

All statistical analyses were performed with Statistical Package for Social Sciences version 22.0 software (SPSS). Data were expressed as mean ± standard error of mean (SEM). A two-tailed significance level was set at $p < 0.05$.

3. Results

3.1. Lis1 KD hampered cell migration NIH3T3 cells

To investigate the role of Lis1 in cell migration, we examined the effects of Lis1 KD on motility of NIH3T3 cells, a commonly used cell line from mouse fibroblasts for migration studies. Cells cultured on collagen were transfected with plasmids expressing green fluorescent protein (GFP) along with short hairpin RNA (shRNA) targeting *Lis1* gene (shLis1) or scrambled control shRNA (shCtrl) [14] for 24 h. The transfected cells were then observed by time-lapse fluorescence microscopy for up to 2 h (Fig. 1A). While control cells exhibited ability to freely migrate, the cells transfected with shLis1 showed significant decreases in the rate (shLis1: 0.23 ± 0.03 μm/min, $n = 37$ cells vs shCtrl: 0.34 ± 0.04 μm/min, $n = 35$ cells; $p = 0.000146$, student's *t*-test; Fig. 1B) and velocity (shLis1: 0.10 ± 0.01 μm/min, vs shCtrl: 0.18 ± 0.02 μm/min; $p = 0.0043$, student's *t*-test; Fig. 1C) of migration. However, Lis1 knockdown (KD) did not affect the persistence of the migration (Fig. 1D), suggesting a minimal effect on the directionality of migration. These results demonstrated that Lis1 KD could cause defects in the rate of migration of NIH3T3 cells.

3.2. Lis1 KD reduced cellular traction force during migration

During cell migration, traction stress is generated to propel the cell body forward [22]. Thus, we postulated that cell motility defects by Lis1 KD may be associated with changes in cellular traction force, which can be measured by TFM [21,24]. NIH3T3 cells were cultured on collagen-coated PAA gel of ~8.8 kPa stiffness embedded with 200-nm fluorescent polystyrene beads. The transfected cells and fluorescent beads near the surface were imaged through time. The gel deformation was detected by the difference in the particle positions during migration compared to those after removal of cells with NaOH (Fig. 2A). The magnitude and vector of bead displacements were measured by PIV algorithm (Fig. 2B; Suppl Fig. 1) [21,24]. Using particle displacements and the elastic modulus, the map of traction stress generated by the cells was calculated (Fig. 2C).

In control cells, the time course of traction force showed that the traction force was exerted on the protruding and retracting regions of cells (Fig. 2C). In cells transfected with shLIS1, the magnitude of total traction force was significantly reduced into one-half of the control cells (untransfected: $1.86 \pm 0.20 \times 10^5$ pN, $n = 6$; shCtrl: $2.10 \pm 0.11 \times 10^5$ pN, $n = 7$; shLis1: $0.99 \pm 0.13 \times 10^5$ pN, $n = 10$; $p < 0.01$; One-way ANOVA; Fig. 2D). The same trend was also observed in the magnitude of average traction stress (untransfected: 149 ± 16 pN/μm^2; shCtrl: 175 ± 18 pN/μm^2; shLis1: 92 ± 12 pN/μm^2, $p < 0.05$; One-way ANOVA; Fig. 2E). Of note, Lis1 knockdown did not affect the cell size (untransfected: 1260 ± 92 μm^2; shCtrl: 1272 ± 138 μm^2; shLis1: 1081 ± 84 μm^2; untransfected vs. shLis1, $p = 0.741$; shCtrl vs. shLis1, $p = 0.588$; One-way ANOVA; Fig. 2F). These results indicated that Lis1 KD could reduce the traction force and stress in NIH3T3 cells during migration.

3.3. Lis1 KD altered cytoskeleton organizations

In order to investigate how Lis1 affects cell motility and traction force, we examined the structures of cytoskeleton, including microtubules and actin filaments. NIH3T3 cells transfected with shCtrl or shLis1 for 24 h were stained with α-tubulin and imaged by confocal microscopy. We observed decreased signals of filamentous microtubule structures in shLis1 compared to those in the

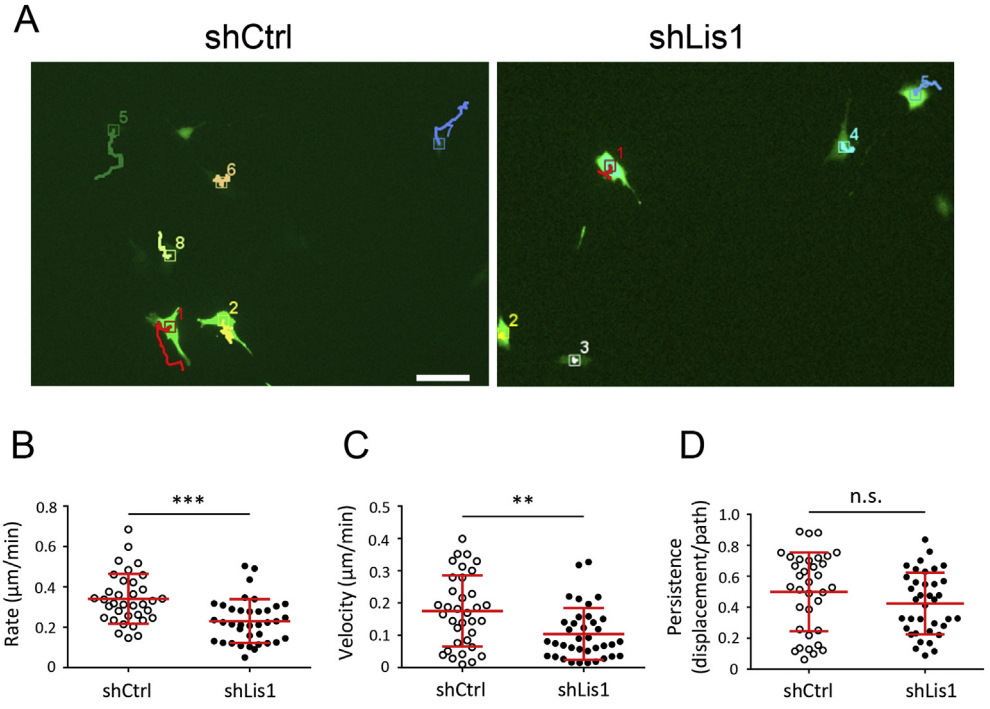

Fig. 1. NIH3T3 cells display a decrease in motility after treatment with Lis1 shRNA.
(A) NIH3T3 cells transfected with shCtrl or shLis1 (green) overlaid with the traces of migration over 2 h of recording. Distance of migration was reduced in cells transfected with shLis1. Bar = 50 μm. (B) Scattered dot plot showing the average rate of cell migration. (C) Scatter dot plot showing the velocity of migration over the 2 h of recording. Both average rate and velocity were significantly decreased by Lis1 KD. (D) Scatter dot plot showing no significant difference in the persistence of migration over the 2 h of recording. Each dot represent one cell. **: $p < 0.01$; ***: $p < 0.001$; Student's *t*-test. Error bars represent standard deviation (S.D.). (For interpretation of the references to colour in this figure legend, the reader is referred to the Web version of this article.)

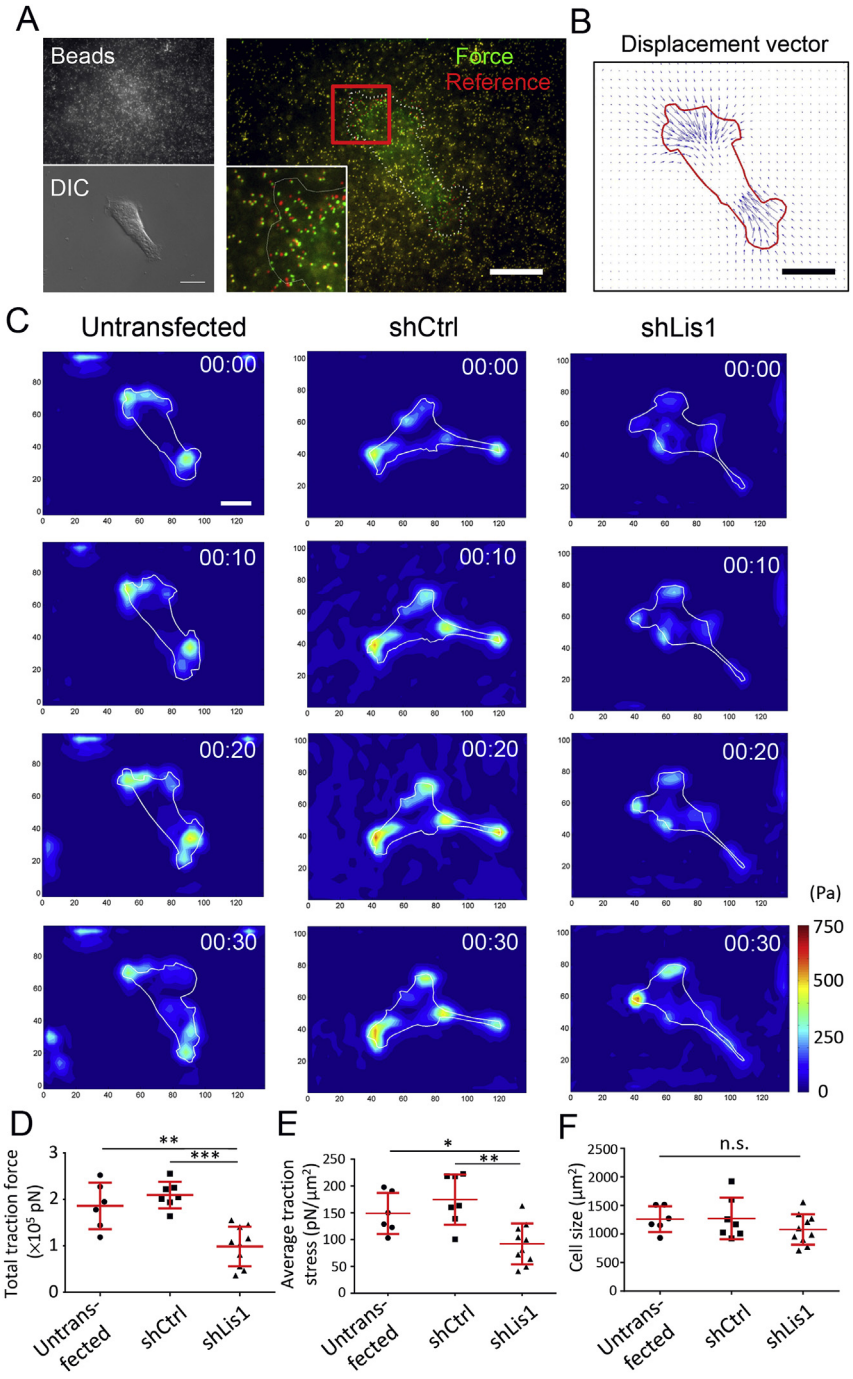

Fig. 2. Lis1 KD decreases cellular traction force during migration of NIH3T3 cells measured by TFM.
(A) Fluorescent image of beads embedded in PAA gel and DIC image of a NIH3T3 cell cultured on top. The deformation of the gel during migration was detected by comparing the bead positions under the cellular traction (green) and after the cells had been removed (red). Bar = 20 μm. (B) Displacement vector map of the fluorescent bead under cellular traction force. The red line outlines the cell boundary of the cell in (A). (C) Heat maps of the traction force magnitude during the migration of untransfected cells and cells transfected with shCtrl or shLis1. The traction force was mainly exerted on the protruding and retracting regions of cells. The white lines outline the cell boundaries. Time is indicated as hr:min. Bar = 20 μm. (D) Scattered dot plot showing a decrease in the magnitude of traction force in shLis1-transfected cells. (E) Scattered dot plot showing that Lis1 KD reduced the average traction stress. (F) Scattered dot plot showing no difference in average cell size among all 3 groups. *: $p < 0.05$; **: $p < 0.01$; ***: $p < 0.001$; One-way ANOVA test. Error bars represent S.D. (For interpretation of the references to colour in this figure legend, the reader is referred to the Web version of this article.)

surrounding untranfected cells or cells transfected with shCtrl (Fig. 3A), consistent with previous observations in embryonic fibroblasts from *Lis1*$^{+/-}$ mouse [11]. We also imaged actin filaments (F-actin) labeled with phalloidin and found that, while F-actin was enriched at the lamellipodia in control cells, Lis1 KD reduced the signal of F-actin at these areas (Fig. 3B). These results suggest that downregulation of Lis1 indeed affects the structures of microtubules and actin filaments.

3.4. Lis1 KD decreased focal adhesion at cell periphery

Since we observed that Lis1 KD reduced traction force, which is

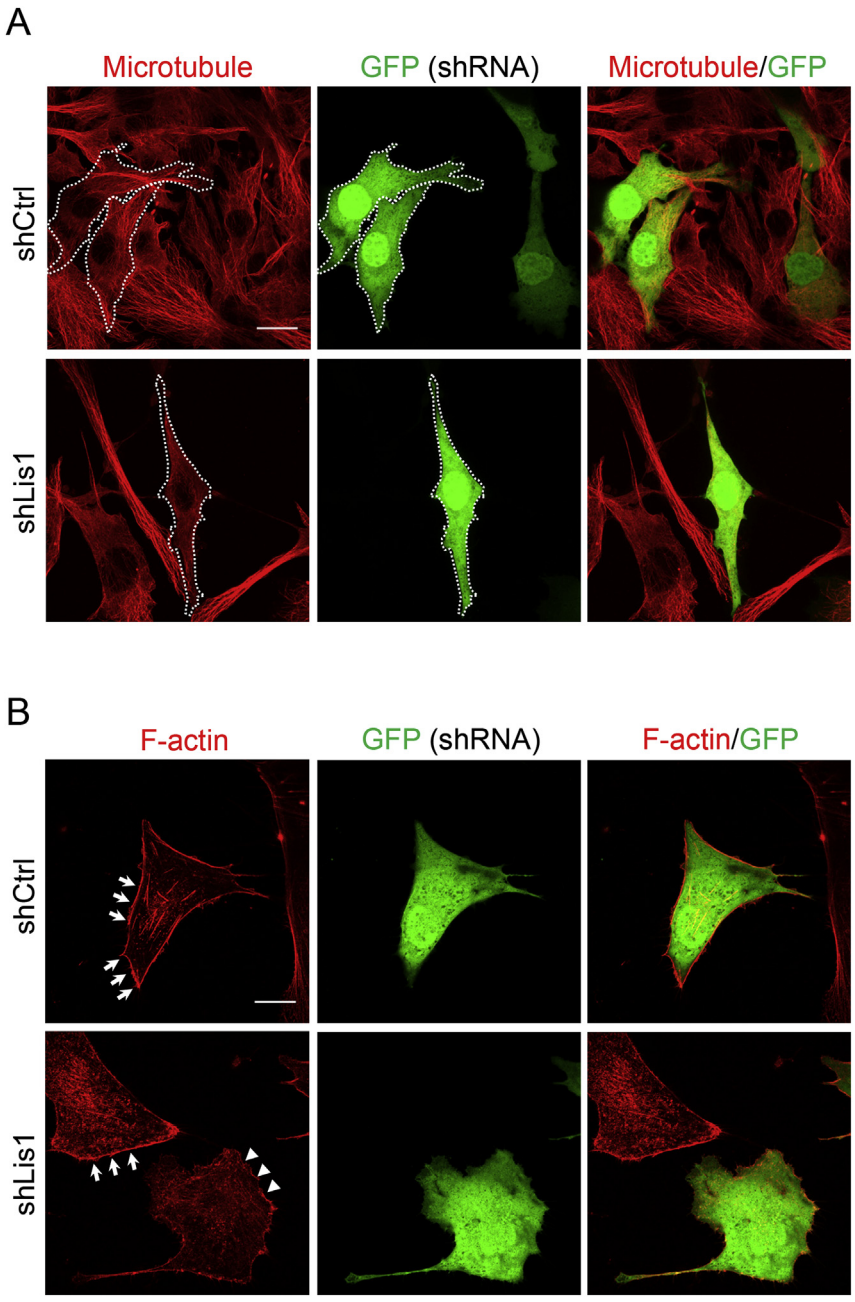

Fig. 3. Lis1 KD alters structures of microtubule and F-actin in NIH3T3 cells.
(A) Immunofluorescence staining of microtubules (red) in NIH3T3 cells expressing shCtrl or shLis1 (green). Lines of microtubules are apparent in control cells while a decreased signal was observed in Lis1 KD cells. (B) F-actin staining by phalloidin (red) in cells transfected with shCtrl or shLIS1 (green). In control cells, concentrated F-actin signal was found at the edge of cells (arrows). In Lis1 KD cells, the signal was largely reduced (arrowheads). Bar = 20 μm. (For interpretation of the references to colour in this figure legend, the reader is referred to the Web version of this article.)

transduced through cell-ECM adhesions, it is possible that focal adhesions against ECM may also be affected. To investigate this possibility, cells transfected with shCtrl or shLis1 for 24 h were stained with paxillin antibody for focal adhesions (Fig. 4A). Focal adhesions were imaged with total internal reflection fluorescent (TIRF) microscopy.

We found that the total number of focal adhesions in each cell was slightly decreased in Lis1 KD cells, although it did not reach a significant difference (shCtrl: 51.7 ± 5.3, $n = 12$ cells; shLis1: 39.5 ± 7.4, $n = 8$ cells; $p = 0.187$, Student's t-test; Fig. 4B). However, the number of focal adhesion within 4 μm from the edge of cells was significantly lower in Lis1 KD cells (shCtrl: 26.9 ± 2.8; shLis1: 13.3 ± 2.5; $p = 0.003$, Student's t-test; Fig. 4C). Interestingly, the average size of each focal adhesion was not affected by Lis1 shRNA (shCtrl: 0.76 ± 0.02 μm^2; shLis1: 0.78 ± 0.03 μm^2; $p = 0.473$, Mann-Whitney U test; Fig. 4D). These results suggest that Lis1 KD specifically affects the number of focal adhesion at cell periphery, which may in turn affect traction force transduction.

4. Discussion

Previous studies have shown that the migration abilities are significantly reduced in cerebellar granule cells and fibroblasts from *Lis1*$^{+/-}$ mice [15]. Consistent with this finding, Lis1 RNAi

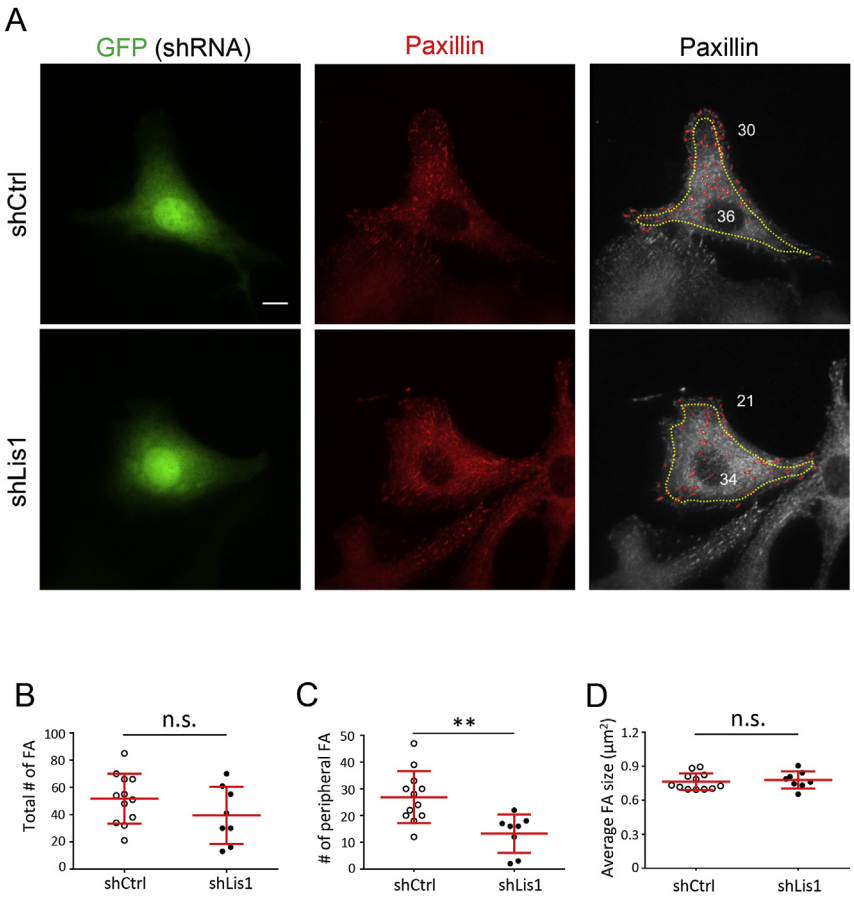

Fig. 4. TIRF microscopy reveals a decrease in focal adhesions at cell periphery by Lis1 KD.
(A) TIRF images of NIH3T3 cells transfected with shCtrl or shLis1 (green, left column) and stained with *anti*-paxillin antibody (red, middle column). Distribution of focal adhesions (red outlines, right column) was analyzed according to the distance to the cell boundary. Numbers indicate the focal adhesions found within or outside 4 μm range (yellow dotted line) from the cell boundaries. Bar = 10 μm. (B) Scattered dot plot showing no change in the total number of focal adhesions in each cell. (C) Scattered dot plot indicating a decrease in the number of adhesions at cell periphery. (D) Scattered dot plot showing that the average size of each focal adhesion was not affected by Lis1 KD. FA: focal adhesions. **: $p < 0.01$; Student's *t*-test. Error bars represent S.D. (For interpretation of the references to colour in this figure legend, the reader is referred to the Web version of this article.)

blocks the motility of cortical neurons during brain development [14,25]. Here we show that Lis1 KD in fibroblasts leads to a significant decrease in both cell migration and traction force generation. This phenotype may result from defects in regulating the organizations of cytoskeleton and focal adhesions.

LIS1 has been shown to play multiple roles in regulating cytoskeleton organization during mitosis, morphogenesis and migration [26,27]. First, Lis1 can bind to tubulin and reduce microtubule catastrophe *in vitro* [28]. In the embryonic fibroblasts from *Lis1*$^{+/-}$ mice, reduced Lis1 results in disorganization of microtubules [11]. In *Dictyostelium*, Lis1 dysfunction alters the microtubule dynamics [29]. These results suggest that Lis1 may regulate microtubule dynamics, consistent with our observations.

Second, Lis1 forms a complex with cytoplasmic dynein [10–12,30] and dynein-associated proteins, such as dynactin, Nde1 [31], and Ndel1 [10,32]. Lis1 can modulate dynein function through promoting the ATPase activity of dynein [33,34]. Lis1 and Nde1 prolong dynein-microtubule interaction during the dynein power stroke *in vitro* [35], leading to better summation of forces generated by multiple cytoplasmic dyneins and enhanced duration of force output. Lis1 and Nde1/Ndel1 also enhance sustained force production of dynein in microtubule-associated lipid droplets in COS1 cells [36].

Furthermore, Lis1 forms a complex with Cdc42 and IQGAP1, a stabilizer for the active GTP-bound form of Cdc42, along with microtubule plus-end protein Clip170 at the cell cortex. Lis1 modulates IQGAP1 and CLIP-170 distribution and neuronal motility in primary cultured neurons [37]. *Lis1*$^{+/-}$ cerebellar granule cells display abnormalities of the actin filaments at the tips of processes, possibly through dysregulation of Rac1, Cdc42, and RhoA activities [15]. Consistent with these results, Lis1 dysfunction also leads to reduced actin filament content and disrupted actin dynamics in *Dictyostelium* [29].

Disorganization and dysregulation of cytoskeleton, including microtubules and actin filaments, as well as dynein motor functions, may in turn affect focal adhesion formation and traction force production. Consistent with this hypothesis, Lis1 has been found to localize at the cell cortex of mitotic MDCK cells, along with dynein and dynactin complex [12]. Overexpression of LIS1 alters the distribution of dynein/dynactin at the cortices and affects the association of dynactin with microtubule plus ends [12]. Based on these studies and our current results, we therefore propose that Lis1 may affect microtubules and actin filaments at the cell cortex. These effects may in turn influence the formation of focal adhesion at cell periphery and traction force generation.

In conclusion, our current study with traction force microscopy indicates that loss of Lis1 function reduces traction force production during cell migration through dysregulation of cytoskeletal components and focal adhesion. These results provide valuable information for our understanding in the mechanisms for traction

force generation during cell migration.

Acknowledgements

We appreciate Dr. Jean-Cheng Kuo (NYMU) for her helpful comments and suggestions. This work was supported by Academia Sinica (AS-NB-012), the Ministry of Science and Technology (101-2320-B-010-077-MY2, 103-2628-B-010-002-MY3, 104-2633-H-010-001, 105-2633-B-009-003, and 106-2628-B-010-002-MY3), Taiwan National Health Research Institutes (NHRI-EX103-10314NC), and Veterans General Hospitals-University System of Taiwan (VGHUST107-G7-1-2).

Transparency document

Transparency document related to this article can be found online at https://doi.org/10.1016/j.bbrc.2018.02.151.

Appendix A. Supplementary data

Supplementary data related to this article can be found at https://doi.org/10.1016/j.bbrc.2018.02.151.

References

[1] T. Mammoto, D.E. Ingber, Mechanical control of tissue and organ development, Development 137 (2010) 1407–1420, https://doi.org/10.1242/dev.024166.
[2] G. Reig, E. Pulgar, M.L. Concha, Cell migration: from tissue culture to embryos, Development 141 (2014) 1999–2013, https://doi.org/10.1242/dev.101451.
[3] P. Friedl, D. Gilmour, Collective cell migration in morphogenesis, regeneration and cancer, Nat. Rev. Mol. Cell Biol. 10 (2009) 445–457, https://doi.org/10.1038/nrm2720.
[4] P. Martin, Wound healing–aiming for perfect skin regeneration, Science 276 (1997) 75–81.
[5] S. Iden, J.G. Collard, Crosstalk between small GTPases and polarity proteins in cell polarization, Nat. Rev. Mol. Cell Biol. 9 (2008) 846–859, https://doi.org/10.1038/nrm2521.
[6] R. Li, G.G. Gundersen, Beyond polymer polarity: how the cytoskeleton builds a polarized cell, Nat. Rev. Mol. Cell Biol. 9 (2008) 860–873, https://doi.org/10.1038/nrm2522.
[7] S. Munevar, Y. Wang, M. Dembo, Traction force microscopy of migrating normal and H-ras transformed 3T3 fibroblasts, Biophys. J. 80 (2001) 1744–1757.
[8] K.A. Beningo, M. Dembo, I. Kaverina, J.V. Small, Y.L. Wang, Nascent focal adhesions are responsible for the generation of strong propulsive forces in migrating fibroblasts, J. Cell Biol. 153 (2001) 881–888.
[9] Y. Aratyn-Schaus, P.W. Oakes, M.L. Gardel, Dynamic and structural signatures of lamellar actomyosin force generation, Mol. Biol. Cell 22 (2011) 1330–1339, https://doi.org/10.1091/mbc.E10-11-0891.
[10] S. Sasaki, A. Shionoya, M. Ishida, M.J. Gambello, J. Yingling, A. Wynshaw-Boris, S. Hirotsune, A LIS1/NUDEL/cytoplasmic dynein heavy chain complex in the developing and adult nervous system, Neuron 28 (2000) 681–696.
[11] D.S. Smith, M. Niethammer, R. Ayala, Y. Zhou, M.J. Gambello, A. Wynshaw-Boris, L.H. Tsai, Regulation of cytoplasmic dynein behaviour and microtubule organization by mammalian Lis1, Nat. Cell Biol. 2 (2000) 767–775, https://doi.org/10.1038/35041000.
[12] N.E. Faulkner, D.L. Dujardin, C.Y. Tai, K.T. Vaughan, C.B. O'Connell, Y. Wang, R.B. Vallee, A role for the lissencephaly gene LIS1 in mitosis and cytoplasmic dynein function, Nat. Cell Biol. 2 (2000) 784–791, https://doi.org/10.1038/35041020.
[13] O. Reiner, R. Carrozzo, Y. Shen, M. Wehnert, F. Faustinella, W.B. Dobyns, C.T. Caskey, D.H. Ledbetter, Isolation of a Miller-Dieker lissencephaly gene containing G protein beta-subunit-like repeats, Nature 364 (1993) 717–721, https://doi.org/10.1038/364717a0.
[14] J.W. Tsai, Y. Chen, A.R. Kriegstein, R.B. Vallee, LIS1 RNA interference blocks neural stem cell division, morphogenesis, and motility at multiple stages, J. Cell Biol. 170 (2005) 935–945, https://doi.org/10.1083/jcb.200505166.
[15] S.S. Kholmanskikh, J.S. Dobrin, A. Wynshaw-Boris, P.C. Letourneau, M.E. Ross, Disregulated RhoGTPases and actin cytoskeleton contribute to the migration defect in Lis1-deficient neurons, J. Neurosci. 23 (2003) 8673–8681.
[16] D.L. Dujardin, L.E. Barnhart, S.A. Stehman, E.R. Gomes, G.G. Gundersen, R.B. Vallee, A role for cytoplasmic dynein and LIS1 in directed cell movement, J. Cell Biol. 163 (2003) 1205–1211, https://doi.org/10.1083/jcb.200310097.
[17] N.R. Morris, Nuclear migration. From fungi to the mammalian brain, J. Cell Biol. 148 (2000) 1097–1101.
[18] A. Swan, T. Nguyen, B. Suter, Drosophila Lissencephaly-1 functions with Bic-D and dynein in oocyte determination and nuclear positioning, Nat. Cell Biol. 1 (1999) 444–449, https://doi.org/10.1038/15680.
[19] J.R. Geiser, E.J. Schott, T.J. Kingsbury, N.B. Cole, L.J. Totis, G. Bhattacharyya, L. He, M.A. Hoyt, Saccharomyces cerevisiae genes required in the absence of the CIN8-encoded spindle motor act in functionally diverse mitotic pathways, Mol. Biol. Cell 8 (1997) 1035–1050.
[20] A.K. Harris, P. Wild, D. Stopak, Silicone rubber substrata: a new wrinkle in the study of cell locomotion, Science 208 (1980) 177–179.
[21] Y.L. Wang, R.J. Pelham Jr., Preparation of a flexible, porous polyacrylamide substrate for mechanical studies of cultured cells, Methods Enzymol. 298 (1998) 489–496.
[22] M. Dembo, Y.L. Wang, Stresses at the cell-to-substrate interface during locomotion of fibroblasts, Biophys. J. 76 (1999) 2307–2316, https://doi.org/10.1016/S0006-3495(99)77386-8.
[23] E. Meijering, O. Dzyubachyk, I. Smal, Methods for cell and particle tracking, Methods Enzymol. 504 (2012) 183–200, https://doi.org/10.1016/B978-0-12-391857-4.00009-4.
[24] H.H. Lee, H.C. Lee, C.C. Chou, S.S. Hur, K. Osterday, J.C. del Alamo, J.C. Lasheras, S. Chien, Shp2 plays a crucial role in cell structural orientation and force polarity in response to matrix rigidity, Proc. Natl. Acad. Sci. U. S. A. 110 (2013) 2840–2845, https://doi.org/10.1073/pnas.1222164110.
[25] J.W. Tsai, K.H. Bremner, R.B. Vallee, Dual subcellular roles for LIS1 and dynein in radial neuronal migration in live brain tissue, Nat. Neurosci. 10 (2007) 970–979, https://doi.org/10.1038/nn1934.
[26] T. Kawauchi, M. Hoshino, Molecular pathways regulating cytoskeletal organization and morphological changes in migrating neurons, Dev. Neurosci. 30 (2008) 36–46, https://doi.org/10.1159/000109850.
[27] H.M. Moon, A. Wynshaw-Boris, Cytoskeleton in action: lissencephaly, a neuronal migration disorder, Wiley Interdiscip Rev Dev Biol. 2 (2013) 229–245, https://doi.org/10.1002/wdev.67.
[28] T. Sapir, M. Elbaum, O. Reiner, Reduction of microtubule catastrophe events by LIS1, platelet-activating factor acetylhydrolase subunit, EMBO J. 16 (1997) 6977–6984, https://doi.org/10.1093/emboj/16.23.6977.
[29] M. Rehberg, J. Kleylein-Sohn, J. Faix, T.H. Ho, I. Schulz, R. Graf, Dictyostelium LIS1 is a centrosomal protein required for microtubule/cell cortex interactions, nucleus/centrosome linkage, and actin dynamics, Mol. Biol. Cell 16 (2005) 2759–2771, https://doi.org/10.1091/mbc.E05-01-0069.
[30] C.Y. Tai, D.L. Dujardin, N.E. Faulkner, R.B. Vallee, Role of dynein, dynactin, and CLIP-170 interactions in LIS1 kinetochore function, J. Cell Biol. 156 (2002) 959–968, https://doi.org/10.1083/jcb.200109046.
[31] Y. Feng, E.C. Olson, P.T. Stukenberg, L.A. Flanagan, M.W. Kirschner, C.A. Walsh, LIS1 regulates CNS lamination by interacting with mNudE, a central component of the centrosome, Neuron 28 (2000) 665–679.
[32] M. Niethammer, D.S. Smith, R. Ayala, J. Peng, J. Ko, M.S. Lee, M. Morabito, L.H. Tsai, NUDEL is a novel Cdk5 substrate that associates with LIS1 and cytoplasmic dynein, Neuron 28 (2000) 697–711.
[33] M.T. Mesngon, C. Tarricone, S. Hebbar, A.M. Guillotte, E.W. Schmitt, L. Lanier, A. Musacchio, S.J. King, D.S. Smith, Regulation of cytoplasmic dynein ATPase by Lis1, J. Neurosci. 26 (2006) 2132–2139, https://doi.org/10.1523/JNEUROSCI.5095-05.2006.
[34] G. Kerjan, J.G. Gleeson, Genetic mechanisms underlying abnormal neuronal migration in classical lissencephaly, Trends Genet. 23 (2007) 623–630, https://doi.org/10.1016/j.tig.2007.09.003.
[35] R.J. McKenney, M. Vershinin, A. Kunwar, R.B. Vallee, S.P. Gross, LIS1 and NudE induce a persistent dynein force-producing state, Cell 141 (2010) 304–314, https://doi.org/10.1016/j.cell.2010.02.035.
[36] B.J. Reddy, M. Mattson, C.L. Wynne, O. Vadpey, A. Durra, D. Chapman, R.B. Vallee, S.P. Gross, Load-induced enhancement of Dynein force production by LIS1-NudE in vivo and in vitro, Nat. Commun. 7 (2016) 12259, https://doi.org/10.1038/ncomms12259.
[37] S.S. Kholmanskikh, H.B. Koeller, A. Wynshaw-Boris, T. Gomez, P.C. Letourneau, M.E. Ross, Calcium-dependent interaction of Lis1 with IQGAP1 and Cdc42 promotes neuronal motility, Nat. Neurosci. 9 (2006) 50–57, https://doi.org/10.1038/nn1619.